

Identification and characterization of the anti-viral interferon lambda 3 as direct target of the Epstein-Barr virus microRNA-BART7-3p

Juliane Blümke, Marcus Bauer, Christoforos Vaxevanis, Andreas Wilfer, Ofer Mandelboim, Claudia Wickenhauser, Barbara Seliger & Simon Jasinski-Bergner

To cite this article: Juliane Blümke, Marcus Bauer, Christoforos Vaxevanis, Andreas Wilfer, Ofer Mandelboim, Claudia Wickenhauser, Barbara Seliger & Simon Jasinski-Bergner (2023) Identification and characterization of the anti-viral interferon lambda 3 as direct target of the Epstein-Barr virus microRNA-BART7-3p, *Oncolmmunology*, 12:1, 2284483, DOI: [10.1080/2162402X.2023.2284483](https://doi.org/10.1080/2162402X.2023.2284483)

To link to this article: <https://doi.org/10.1080/2162402X.2023.2284483>



© 2023 The Author(s). Published with license by Taylor & Francis Group, LLC.



[View supplementary material](#)



Published online: 27 Nov 2023.



[Submit your article to this journal](#)



Article views: 419



[View related articles](#)



[View Crossmark data](#)

Identification and characterization of the anti-viral interferon lambda 3 as direct target of the Epstein-Barr virus microRNA-BART7-3p

Juliane Blümke^{a*}, Marcus Bauer^{b*}, Christoforos Vaxevanis^a, Andreas Wilfer^{b,c}, Ofer Mandelboim^d, Claudia Wickenhauser^b, Barbara Seliger^{a,e,f}, and Simon Jasinski-Bergner^{a,f}

^aInstitute for Medical Immunology, Martin-Luther-University Halle-Wittenberg, Halle, Germany; ^bInstitute for Pathology, Martin-Luther-University Halle-Wittenberg, Halle, Germany; ^cKrukenberg Cancer Center, University Hospital Halle, Martin-Luther-University Halle-Wittenberg, Halle, Germany; ^dDepartment of Immunology, Faculty of Medicine, The Hebrew University of Jerusalem, Jerusalem, Israel; ^eDepartment of Good Manufacturing Practice (GMP) Development & Advanced Therapy Medicinal Products (ATMP) Design, Fraunhofer Institute for Cell Therapy and Immunology (IZI), Leipzig, Germany; ^fInstitute for Translational Immunology, Brandenburg Medical School (MHB), Brandenburg an der Havel, Germany

ABSTRACT

The human Epstein-Barr virus (EBV), as a member of the human γ herpes viruses (HHV), is known to be linked with distinct tumor types. It is a double-stranded DNA virus and its genome encodes among others for 48 different microRNAs (miRs). Current research demonstrated a strong involvement of certain EBV-miRs in molecular immune evasion mechanisms of infected cells by, e.g., the disruption of human leukocyte antigen (HLA) class Ia and NKG2D functions. To determine novel targets of EBV-miRs involved in immune surveillance, ebv-miR-BART7-3p, an EBV-encoded miR with high expression levels during the different lytic and latent EBV life cycle phases, was overexpressed in human HEK293T cells. Using a cDNA microarray-based comparative analysis, 234 (229 downregulated and 5 upregulated) deregulated human transcripts were identified in ebv-miR-BART7-3p transfectants, which were mainly involved in cellular processes and molecular binding. A statistically significant downregulation of the anti-proliferative and tumor-suppressive hsa-miR-34A and the anti-viral interferon lambda (IFNL3) mRNA was found. The ebv-miR-BART7-3p-mediated downregulation of IFNL3 expression was due to a direct interaction with the IFNL3 3'-untranslated region (UTR) as determined by luciferase reporter gene assays including the identification of the accurate ebv-miR-BART7-3p binding site. The effect of ebv-miR-BART7-3p on the IFNL3 expression was validated both in human cell lines *in vitro* and in human tissue specimen with known EBV status. These results expand the current knowledge of EBV-encoded miRs and their role in immune evasion, pathogenesis and malignant transformation.

ARTICLE HISTORY

Received 28 August 2023
Revised 13 November 2023
Accepted 13 November 2023

KEYWORDS

EBV; EBV target genes; IFNL3; immune escape; microRNA

Introduction

The human Epstein-Barr virus (EBV) exerts a high transmission rate with an incidence of more than 90% of the world population.¹ EBV infection has been linked to distinct solid and hematopoietic malignancies, including nasopharyngeal carcinoma (NPC), gastric adenocarcinoma (GC), classical Hodgkin lymphoma (cHL) and Burkitt lymphoma (BL).²⁻⁶ The double-stranded (ds) DNA EBV genome encodes for >80 genes as well as to date for 48 viral microRNAs (miRs), which are classified depending to their genomic location (BHRF1 and BART) into ebv-miR-BHRFs and ebv-miR-BARTs.^{7,8}


EBV establishes a stable, low-level, lifetime persistent infection in B cells.⁹ Many of the EBV-encoded molecules have a direct impact on the host immune surveillance ranging from viral encoded peptides, proteins and even miRs known to interfere with important immunological processes, like proper cytokine and chemokine signaling, which includes e.g. CXCL-11 downregulation by ebv-miR-BHRF1-3.¹⁰ In

addition, EBV-encoded molecules interfere with the induction of cellular stress molecules with anti-viral functions like the NKG2D ligands.⁸ Furthermore, the immune recognition relevant antigen processing and presentation via classical HLA class Ia molecules is impaired by several EBV-encoded molecules including ebv-miRs, e.g. ebv-miR-BART17 and ebv-miR-BHRF1-3, respectively.¹¹

MiRs are small non-coding RNAs, which bind to their target mRNAs sequence specifically and lead to mRNA decay and/or translational inhibition.^{12,13} Regarding their biological impact on tumors, miRs have been clarified as oncogenic or tumor-suppressive.¹⁴ The fact that EBV expresses virally encoded miRs with immune suppressive and/or oncogenic functions and induces endogenous human oncogenic and/or immune suppressive miRs is of high relevance to understand the molecular processes of EBV-mediated immune evasion and EBV-driven malignant transformation of the infected host cells.

CONTACT Simon Jasinski-Bergner  simon.jasinski-bergner@mhb-fontane.de  Institute for Translational Immunology, Brandenburg Medical School (MHB) Theodor Fontane, Hochstraße 29, Haus 11, 2.OG, Brandenburg an der Havel 14770, Germany

*These Authors are contributed equally for this article.

 Supplemental data for this article can be accessed online at <https://doi.org/10.1080/2162402X.2023.2284483>

© 2023 The Author(s). Published with license by Taylor & Francis Group, LLC.

This is an Open Access article distributed under the terms of the Creative Commons Attribution-NonCommercial License (<http://creativecommons.org/licenses/by-nc/4.0/>), which permits unrestricted non-commercial use, distribution, and reproduction in any medium, provided the original work is properly cited. The terms on which this article has been published allow the posting of the Accepted Manuscript in a repository by the author(s) or with their consent.

To prevent the direct or indirect effects of other EBV-encoded miRs/proteins, the ebv-miR-BART7-3p was separately overexpressed in EBV-negative cells, followed by transcriptome analysis in comparison to an overexpressed control miR leading to 234 differentially expressed genes including the anti-viral cytokine IFNL3 as a novel candidate target of the EBV-encoded ebv-miR-BART7-3p. The direct interaction of ebv-miR-BART7-3p and IFNL3 mRNA was verified by respective molecular biological assays and its expression was also analyzed *in vivo* in human EBV-positive tissue specimens to determine its function in immune evasion of infected host cells as well as its clinical relevance (Supplemental Figure S1).

Materials and methods

Cell lines, cell transfection and electroporation

All human cell lines used in this study were purchased from American Type Culture Collection (ATCC, Manassas, VA, USA). The HCC1937 cells and the HEK293T cells as well as the respective transfectants were cultivated as already described.¹²

For transient transfection of plasmids (pmR-mCherry, Takara, Kusatsu, Japan; Catalog No. 632542; pmirGLO, Promega, Madison, WI, USA, Catalog No. E1330) TurboFect (Thermo Fisher Scientific, Waltham, MA, USA) and for transfection of the miRNA inhibitors (mirVana, Thermo Fisher Scientific) the Neon Electroporator (Thermo Fisher Scientific) were applied.

Flow cytometry, protein extraction, Western blot and ELISA

Flow cytometry was performed as recently described,¹³ with anti-CD19 PE (Clone 4G7, Becton Dickinson, Franklin Lakes, NJ, USA), anti-HLA-ABC-FITC (Clone B9.12.1; Beckman Coulter, Brea, CA, USA) monoclonal antibodies (mAb), as well as the respective isotype controls.

Total protein was extracted with xTractor™ Buffer (Takara) and 50 µg protein/lane was separated on a 12% (V/V) SDS-polyacrylamide gel (Serva Electrophoresis, Heidelberg, Germany). Subsequently, the proteins were transferred into a PVDF membrane (Bio-Rad, Hercules, CA, USA), which was prior activated with methanol (Carl Roth, Karlsruhe, Germany), overnight in a tank blotting system at 100 mA (Bio-Rad). Murine anti-IFNL3 mAb (Clone: 567143; Thermo Fisher Scientific) and the murine anti-β-actin mAb (Clone mAbcam 8226; Abcam, Cambridge, UK) as housekeeping gene were used as primary Ab and as secondary antibody: anti-mouse IgG, HRP-linked antibody was used (Cell Signaling Technology, Danvers, MA, USA).

The anti-IFNL3 ELISA (R&D System Minneapolis, MN, USA) was applied for the IFNL3 detection in the cell culture supernatants of the HEK293T transfectants (48 h after transfection).

Luciferase reporter gene assays

A detailed description of the luciferase reporter gene assays including the determination and deletion of the ebv-miR-BART7-3p binding site within the IFNL3 3'-UTR by fusion PCR is provided within the supplemental material.

RNA extraction, cDNA synthesis, qPCR and cDNA microarrays

For the analysis of miRs, total RNA from cell pellets was extracted using the TRIzol Reagent (Thermo Fisher Scientific) and for RNA extraction from FFPE tissue blocks the MasterPure™ Complete DNA and RNA Purification Kit (Lucigen, Middleton, USA). To quantify IFNL3 mRNA levels by qPCR, the NucleoSpin RNA Mini Kit (MACHEREY-NAGEL, Düren, Germany) was utilized.

Subsequently, cDNA synthesis was performed with RevertAid H Minus Reverse Transcriptase (Thermo Fisher Scientific) and random hexamers. For the detection of the IFNL3 mRNA by qPCR the forward 5'-CCCCAAAAGGAG TCCCTG-3' and reverse 5'-GGTTGCATGACTGGCGGA-3' and for the GAPDH mRNA forward 5'-CAAGGTCAT CCATGACAACCTTTG-3' and reverse 5'-GTCCACCACCCTG TTGCTGTAG-3' (Thermo Fisher Scientific) primers were used.

For miR detection, template specific cDNA syntheses were performed according to Chen et al.¹⁵ using following stem-loop oligonucleotides for reverse transcription: ebv-miR-BART7-3p (5'-GTCGTATCCAGTGCAGGGTCCGAGGTA TTCGCACTGGATACGACCCCTGG-3'), hsa-miR-152-3p (5'-GTCGTATCCAGTGCAGGGTCCGAGGTATTTCGCAC TGGATACGACCCAAGT-3') and hsa-miR-34A-5p (5'-GTCGTATCCAGTGCAGGGTCCGAGGTATTTCGCACTG GATACGACACAACC-3') followed by qPCR analyses using the miR-specific forward primers: qPCR152fw 5'-GCCC TCAGTGCATGACAGA-3', qPCRBART7fw 5'-GCCCCATC ATAGTCCAGTGT-3' and qPCR34Afw 5'-GCCCTGGCAG TGTCTTAGCTGG-3' in combination with the pan-miR-reverse qPCR-primer 5'-GTGCAGGGTCCGAGGT-3', whose binding site is added by the stem-loop primers during template-specific cDNA synthesis.

TRIzol-extracted total RNA of three biological replicates for each transfectant was applied for further transcriptome analyses using the Human HT12v4 microarray chips (Illumina, San Diego, CA, USA), and miR analyses were performed using the Core Unit "DNA technologies" (PD Dr. Knut Krohn, University of Leipzig, Medical Faculty, Germany).

Patient samples

Formalin-fixed and paraffin-embedded (FFPE) tissue specimens from 22 different patients (Table 1) was collected in the period from 2011 to 2022 and archived at the Institute of Pathology, Martin-Luther University Halle-Wittenberg, Halle, Germany, analyzed according to the principles expressed in the Declaration of Helsinki.

Table 1. Characteristics of the FFPE human tissue specimen used.

Disease condition	Tissue	Diagnosis	Number of samples	EBV status	Age (mean)	Sex (male/female)
Infectious	Tonsil	Infectious mononucleosis	3	Positive	14–26 (21)	3/0
Neoplastic	Lymph node	DLBCL	2	Positive	56–67 (62)	1/1
		Plasmoblastic lymphoma	2	Positive	74–84 (80)	1/1
		cHL	3	Positive	17–58 (31)	3/0
	Nasopharynx	mPTLD	2	Positive	70–76 (73)	1/1
		ENKTL	2	Positive	42–60 (56)	2/0
		NPC	2	Positive	44–46(45)	2/0
			7	Negative	33–77 (58)	4/3
Reactive	Lymph node	Reactive lymph node				

The scientific use of the anonymized FFPE slides was approved by the Ethical Committee of the Medical Faculty in Halle, Germany (2017-81). All tissue specimens were taken at the time point of primary diagnosis. Standard morphological and histopathological diagnostics were performed according to the diagnostic criteria of the World Health Organization (WHO) Classification of Tumours of Haematopoietic and Lymphoid Tissues, fourth edition 2017¹⁶ and World Health Organization (WHO) Classification of Head and Neck Tumours 2016.¹⁷

Determination of EBV and IFNL3 by *in situ* hybridization

For EBV-encoded RNA chromogenic *in situ* hybridization (EBER-ISH), a Bond Ready-to-Use ISH EBER Probe (PB0589, Leica Biosystems Nussloch GmbH, Wetzlar, Germany) in combination with Bond Polymer Refine Detection Kit (DS9800-CN, Leica Biosystems Nussloch GmbH, Wetzlar, Germany) was applied on 4 µm thick FFPE tissue slides. The detection was performed on a Bond III automated stainer (Leica Biosystems Nussloch GmbH, Wetzlar, Germany). Positive controls from acute EBV infectious mononucleosis were included for all samples on the same slide. *In situ* hybridization for IFNL3 was also performed on 4 µm thick FFPE tissue slides using an HsIFNL3-O2-C1 probe (1237271-C1, Bio-Techne, MN, USA), the RNAscope Multiplex Fluorescent V2 Assay (323100, Bio-Techne, MN, USA) and Opal 570 Fluorophore (FP1488001KT, Akoya Biosciences) according to the manufacturer's instructions. The expression levels of IFNL3 were analyzed by employing the inform software (Akoya Bioscience), and the mean fluorescence intensities (MFIs) were calculated. As positive and negative controls, paraffin-embedded cell blocks of EBV-positive and -negative B cell lines with proofed IFNL3 expression were used.

Statistical evaluation and software

All statistically significant (two-tailed Mann–Whitney *U* test) values were marked with * ($p < 0.05$), with ** ($p < 0.005$) and with *** ($p < 0.0005$). For statistical analyses and visualization Microsoft Excel 2016 (Microsoft Corporation, Redmond, WA, USA), Prism GraphPad9 (GraphPad Software, San Diego, CA, USA), R 3.3.0+ and RStudio (<https://www.r-project.org/>) were applied.

Results

Ebv-miR-BART7-3p significantly downregulates *IFNL3* mRNA expression

To investigate the impact of *ebv-miR-BART7-3p* on host gene expression, the EBV-negative human cell line HEK293T with an intact HLA class I antigen processing and presentation machinery (APM) was transiently transfected with an *ebv-miR-BART7-3p* expression vector and a control vector encoding for the overexpression of human *hsa-miR-541*.

Indeed, 72 h after transient transfection, a strong statistically significant ($p = 0.0005$) overexpression of *ebv-miR-BART7-3p* was detected when compared to the control vector transfectants (Figure 1a). Subsequently, the *ebv-miR-BART7-3p* and control transfectants were subjected to transcriptome analyses by cDNA microarrays. The significant direct or indirect regulated genes upon the *ebv-miR-BART7-3p* overexpression were visualized as a volcano plot (Figure 1b), with the strongest effect for *IFNL3*. To investigate the biological functions of the *ebv-miR-BART7-3p*, a GO term enrichment analysis with the online database Panther (<http://pantherdb.org>) was performed. The *x*-fold changes were calculated, and cutoffs were defined as <0.85 for downregulation ($n = 229$ genes) and as >1.5 for upregulation ($n = 5$ genes). The annotation clustering of the directly or indirectly downregulated 229 genes, including putative *ebv-miR-BART7-3p* targets, is shown in Figure 1c.

Several genes displaying a reduced expression upon *ebv-miR-BART7-3p* overexpression exhibit known functions in tumor biology and immunology. After the quantification of selected targets by qPCR (data not shown), *IFNL3* was identified as strongest downregulated putative *ebv-miR-BART7-3p* target gene on the mRNA level. *IFNL3* was present in certain annotation clusters demonstrating a strong influence of *ebv-miR-BART7-3p* on important tumor-associated pathways, thereby highlighting *IFNL3* as an interesting target for further investigations. However, there was no differential mRNA expression pattern detectable for genes involved in the *IFNL3* downstream signaling (see Supplemental Table S1). If there are also effects of *ebv-miR-BART7-3p* or any other EBV-encoded (miR) gene at the (protein) level, or on any modifications such as the phosphorylation status, cellular localization, etc. of *IFNL3* downstream genes, including *JAK1*, *STAT1*, *STAT2*, *IRF9*, *TYK2*, *IL10RB* could be addressed in further studies.

The transcripts *hsa-miR-34A*, which is a known tumor suppressor miR¹⁸ and *IFNL3* ($p = 0.0003$), a type III interferon (IFN) with known anti-viral functions in the respiratory tract,¹⁹ were found to be significantly downregulated (Figure 1b).

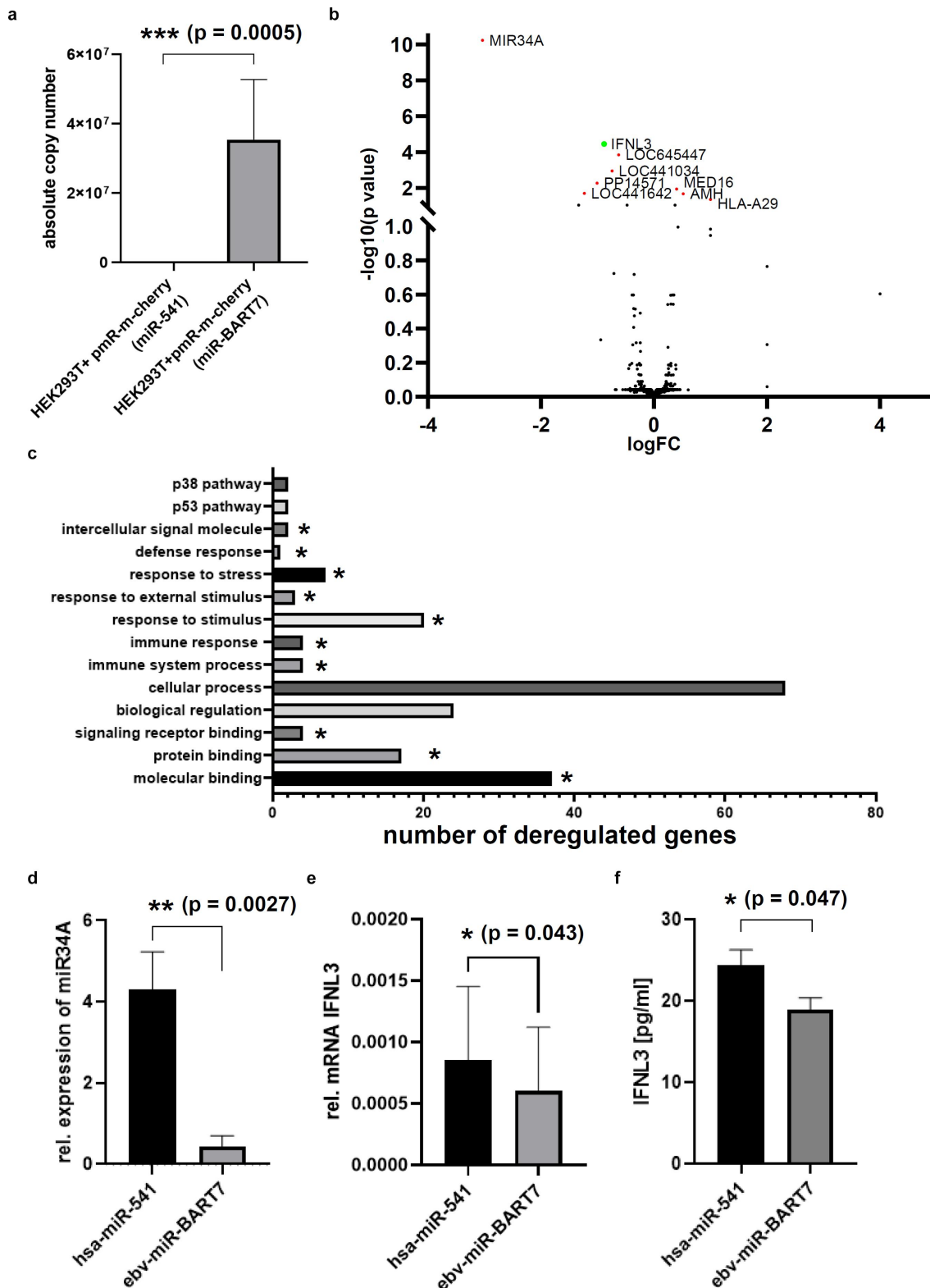


Figure 1. Effects of ebv-miR-BART7-3p overexpression on the transcriptome of HEK293T cells. (a) The expression of ebv-miR-BART7-3p was determined in the respective transfectants by qPCR and presented as absolute copy numbers, overexpression of hsa-miR-541 served as control in transiently transfected HEK293T cells (each $n=6$). (b) cDNA microarray-based transcriptome analysis of ebv-miR-BART7-3p transfectants visualized by a volcano plot. The differential expression pattern was determined and correlated to the control transfectants (hsa-miR-541). (c) The differentially expressed transcripts were subjected to a GO term enrichment analysis using the online database panther (<http://panterdb.org>). IFNL3-containing pathways are labeled with a star. Validation of the two selected and statistically significant downregulated transcripts, in particular hsa-miR-34A and IFNL3, by qPCR ((d) each $n=6$, (e) each $n=3$) and by ELISA ((f) $n=3$).

Indeed, qPCR analyses revealed a statistically significant downregulation of hsa-miR-34A ($p = 0.0027$) and IFNL3 ($p = 0.043$) due to ebv-miR-BART7-3p overexpression in HEK293T

cells (Figure 1d, e). Furthermore, ebv-miR-BART7-3p overexpression resulted in a statistically significant ($p = 0.047$) downregulation of IFNL3 secretion determined by ELISA (Figure 1f).

EBV-positive B cell lymphoma cell lines show a significantly lower IFNL3 expression

To study the interactions between IFNL3 and hsa-miR-34A with ebv-miR-BART7-3p, human EBV-positive (EB1, DAUDI, RAJI) and EBV-negative (BV173, CA46, DG75) B lymphoma cell lines were analyzed. The CD19 and HLA-ABC cell surface expression was analyzed using flow cytometry (Figure 2a). K562 cells served as negative controls for CD19 and HLA class I markers. Furthermore, no correlation between the EBV status and HLA class I expression was found. The lack of HLA class I surface expression on DAUDI cells is due to a known β_2 -microglobulin (β_2 -m) defect.²⁰ The ebv-miR-

BART7-3p expression within the selected B cell lines was determined by qPCR and only detectable within the EBV-positive cell lines with EB1 and RAJI expressing higher ebv-miR-BART7-3p levels than DAUDI cells (Figure 2b). It is noteworthy that the HEK293T transfectants expressed ebv-miR-BART7-3p comparable to EB1 and RAJI cells, thereby proving the functionality and its comparability of the vector-based expression system to mimic viral expression values. As shown in Figure 2b, the different B cell lines expressed the endogenous hsa-miR-152 at equal levels, thereby excluding differences in the miR processing machinery within the different applied cell lines.

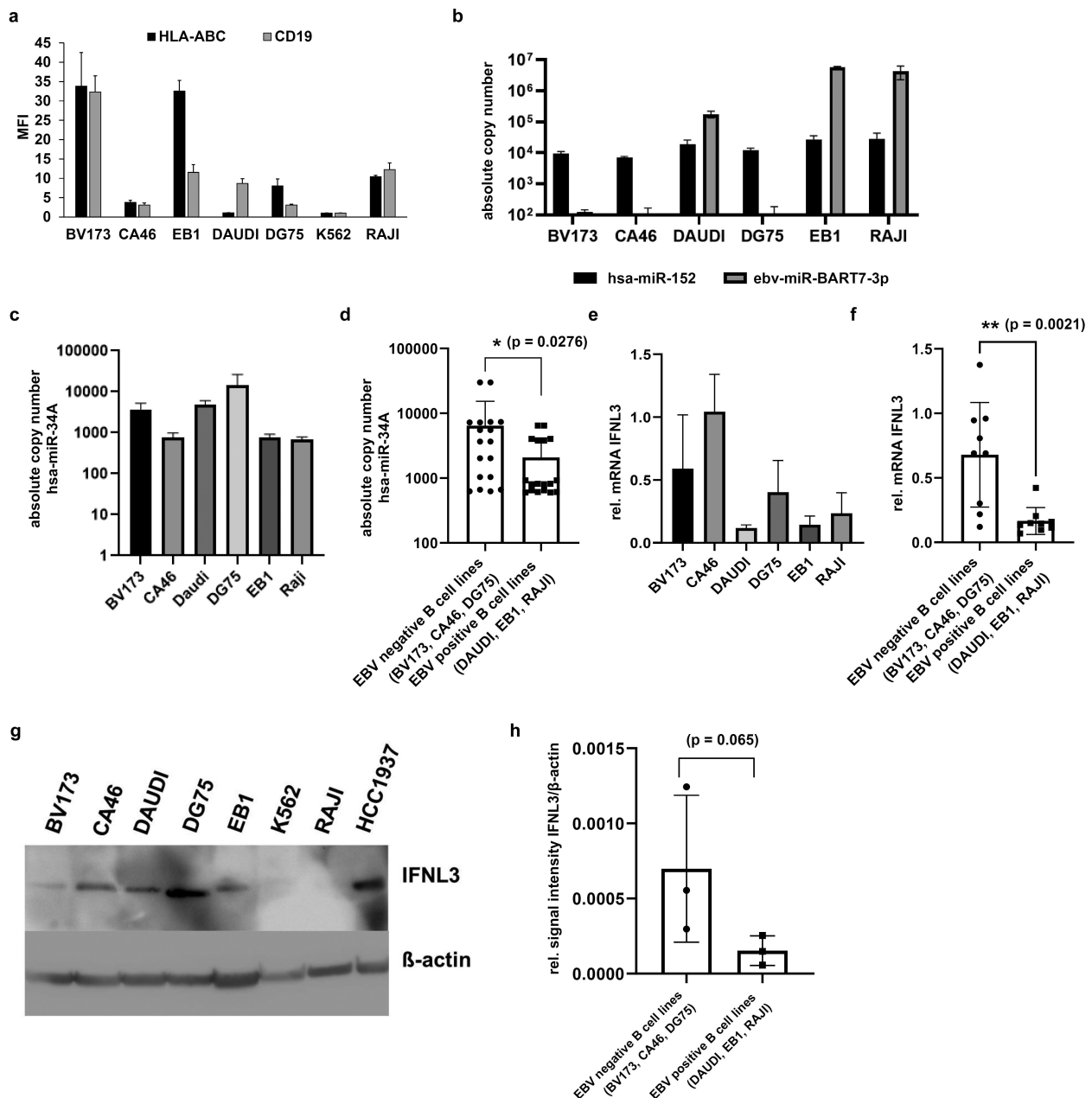


Figure 2. Characterizing the expression of ebv-miR-BART7-3p, hsa-miR-34A and IFNL3 in EBV-positive and EBV-negative B cell lines. (a) A set of EBV-positive and EBV-negative B cell lines was analyzed for HLA-ABC and CD19 surface expression by flow cytometry using K562 cells as a negative control for both markers (each $n=3$). (b) The ebv-miR-BART7-3p expression was determined in different human B cell lymphoma cell lines by qPCR using hsa-miR-152 as endogenous control (each $n=6$). (c, d) Expression analysis of ebv-miR-BART7-3p downregulated hsa-miR-34A determined by qPCR (each $n=6$) and the results are presented in bar charts as absolute copy numbers. In analogy, the statistically significant downregulated IFNL3 was quantified by qPCR ((e, f) each $n=3$) and by Western blot in various B cell lines with known EBV status (g, h).

In addition, the expression of the two ebv-miR-BART7-3p downregulated target genes, namely hsa-miR-34A and IFNL3, was also validated in the B cell lymphoma cell lines with known EBV status using qPCR.

The hsa-miR-34A ($p = 0.0276$) (Figure 2c, d) and the IFNL3 mRNA ($p = 0.0021$) (Figure 2e, f) were statistically significantly downregulated in the EBV-positive B cell lymphoma cell lines when compared to the EBV-negative B cell lymphoma cell lines determined by qPCR. The low IFNL3 mRNA levels in EBV-positive B cell lines were also accompanied by reduced IFNL3 protein levels as determined by Western blot analyses, which was almost statistically significant ($p = 0.065$) (Figure 2g, h).

Underlying mechanisms of ebv-miR-BART7-3p-mediated downregulation of IFNL3

While the ebv-miR-BART7-3p-mediated downregulation of the tumor suppressive endogenous hsa-miR-34A is due to an unknown indirect mechanism, the observed downregulation of the anti-viral IFNL3 mRNA and protein by ebv-miR-BART7-3p overexpression is achieved by direct binding of ebv-miR-BART7-3p to the IFNL3 3'-UTR. Luciferase reporter gene

assays revealed that the wild-type (wt) sequence of the IFNL3 3'-UTR leads to a statistically significant reduced luciferase activity upon ebv-miR-BART7-3p overexpression ($p = 0.023$) when compared to a control miR (Figure 3a). This was underlined by *in silico* prediction of the ebv-miR-BART7-3p binding site and calculation of the free energy of this interaction using RNAhybrid (Figure 3b).²¹

Deletion of the *in silico* predicted ebv-miR-BART7-3p binding site within the IFNL3 3'-UTR was approved by sequence alignment after Sanger sequencing (Figure 3c) and did not furthermore allow a statistically significant ($p = 0.7258$) downregulation of the luciferase reporter gene activity upon ebv-miR-BART7-3p overexpression when compared to the control miR (Figure 3d), thereby confirming the precise ebv-miR-BART7-3p binding site.

To validate the influence of ebv-miR-BART7-3p on the IFNL3 expression, the two EBV-positive B cell lines EB1 and RAJI, which exerted the highest ebv-miR-BART7-3p expression levels (Figure 2b), were transfected with a sequence-specific inhibitor of ebv-miR-BART7-3p. As determined by qPCR, the ebv-miR-BART7-3p inhibitor caused a statistically significant downregulation of ebv-miR-BART7-3p levels in EB1 ($p = 0.0487$) and RAJI ($p = 0.0001$) cells, which was

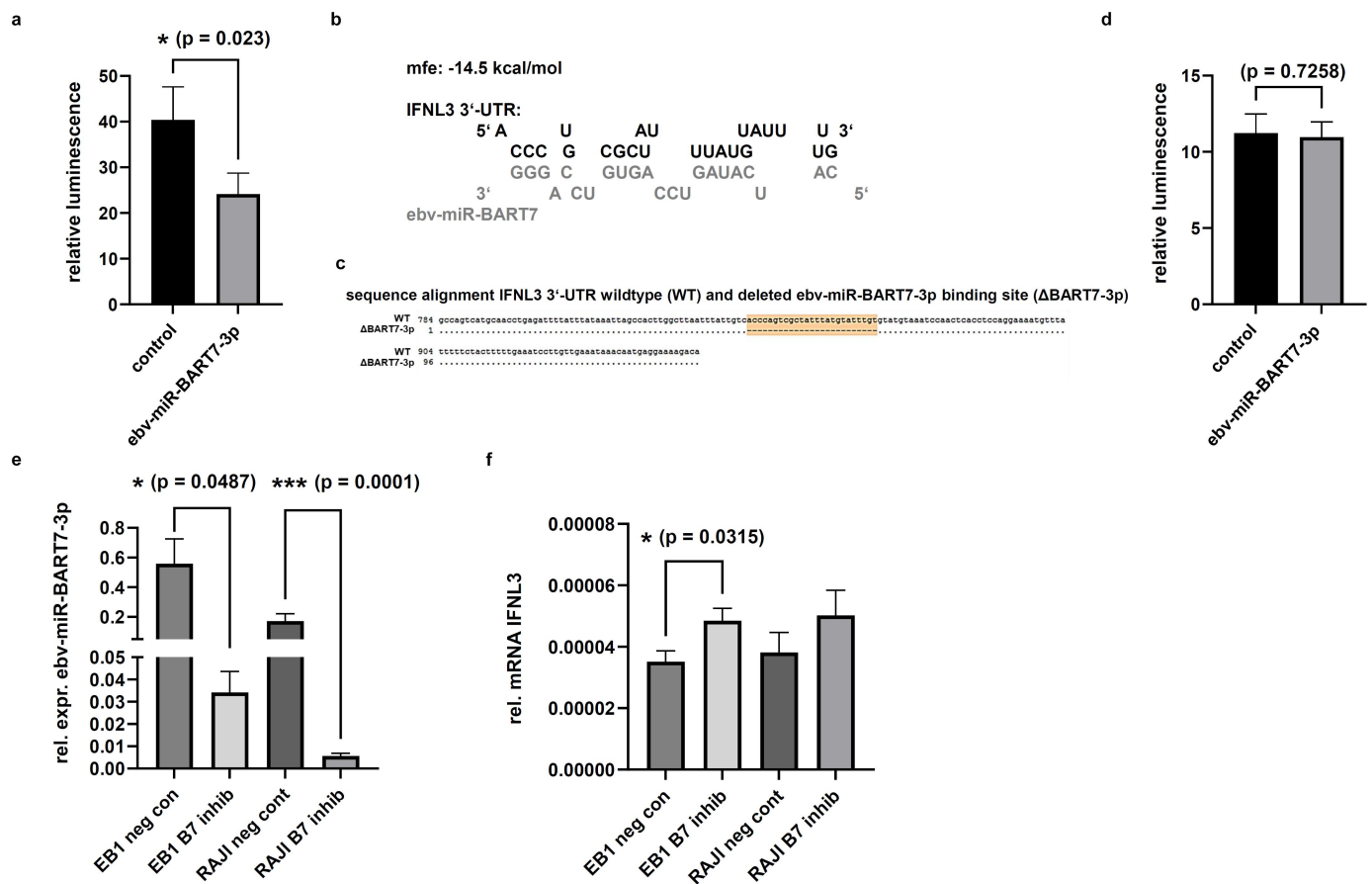


Figure 3. Identification of the direct interaction between ebv-miR-BART7-3p and its target IFNL3 including the determination of its precise binding site within the IFNL3 3'-UTR. (a) Determination of the luciferase reporter gene activity: IFNL3 wild-type 3'-UTR in combination with control ($n=3$) and ebv-miR-BART7-3p ($n=3$) overexpression. (b) Deletion of the *in silico* predicted ebv-miR-BART7-3p binding site within the IFNL3 3'-UTR obtained by RNAhybrid²¹ followed by sequence alignment of its deletion after Sanger sequencing (c). (d) Determination of the luciferase reporter gene activity: IFNL3 mutated 3'-UTR lacking the *in silico* predicted ebv-miR-BART7-3p binding site with control ($n=3$) and ebv-miR-BART7-3p overexpression ($n=3$). (e) Validation of the applied ebv-miR-BART7-3p inhibitors in EBV positive B cell lines by qPCR ($n=3$). (f) Analysis of IFNL3 mRNA levels in the ebv-miR-BART7-3p inhibitor treated EBV-positive B cell lines by qPCR ($n=3$).

accompanied by statistically significant enhanced IFNL3 mRNA levels in EB1 cells ($p = 0.0315$) and to a lesser extent for RAJI cells, but not statistically significant (Figure 3e, f).

Validation of *ebv-miR-BART7-3p* and *IFNL3* interaction in EBV-positive and EBV-negative human tissues

For a translation of these *in vitro* results into *in vivo* human tissue specimen, the expression of *ebv-miR-BART7-3p* was quantified in human EBV-positive FFPE tissue specimen with proofed EBV status determined by EBER *in situ* hybridization (EBER-ISH). The expression levels of *ebv-miR-BART7-3p* (11 EBV-positive lymphoma, two EBV-positive NPC and three tonsils with infectious mononucleosis) were significantly higher ($p = 0.0002$) in EBV-positive samples when compared to EBV-negative samples, which lack or showed only marginal *ebv-miR-BART7-3p* expression in all cases (Figure 4a). Due to the high expression levels of *ebv-miR-BART7-3p* in FFPE specimen of EBV-positive human lymph nodes and the inverse expression of *IFNL3* (Figure 2), the *IFNL3* gene product expression was determined in these FFPE specimens. In analogy to the EBER-ISH (Figure 4b, c), *IFNL3* mRNA was also quantified by RNA *in situ* hybridization (Figure 4d, e) after the establishment of the staining protocol in B cell lines using cell blocks. Representative results of *IFNL3 in situ* hybridization are shown from the same EBV-positive (Figure 4d) and from

the same EBV-negative-reactive lymph node (Figure 4e), which were applied for the EBER-ISH.

Indeed, the EBV-positive tissue specimen had strong statistically significant decreased *IFNL3* mRNA levels (Figure 4f, $p = 0.0004$) when compared to the EBV-negative cases, but even *ebv-miR-BART7-3p* high-expressing tissues (separated by median value ≥ 0.01 for the relative copy numbers) had statistically significant lower *IFNL3* mRNA levels than *ebv-miR-BART7-3p* low-expressing tissues (< 0.01 relative copy numbers; Figure 4g, $p = 0.0482$). These data prove the functionality of this regulatory axis between *ebv-miR-BART7-3p* and *IFNL3* mRNA in human EBV-infected tissue specimen.

Discussion

The ability of EBV to establish a life-long persistent latency in infected host cells is a characteristic feature of herpesviruses. It persists quiescently in resting memory B cells thereby successfully escaping from immune surveillance.⁹ Certain situations allow the entry into the lytic life cycle phase, e.g. chronic immune suppression, but also during the differentiation of the infected memory B cells into plasma cells. Despite EBV hiding only in a small number of infected host cells, it avoids the detection and elimination by immune effector cells by further molecular mechanisms, which have been recently reviewed by the authors.⁸

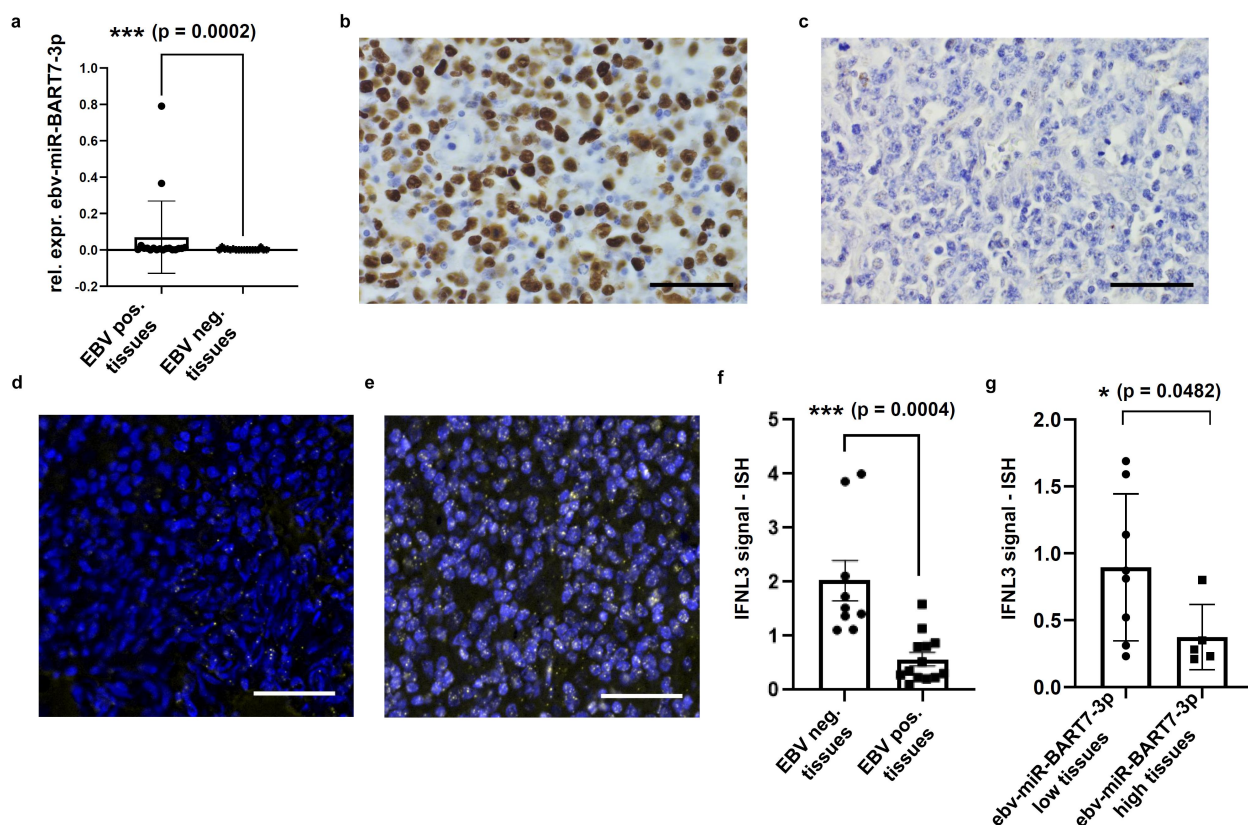


Figure 4. *In vivo* validation of the *ebv-miR-BART7-3p*-mediated *IFNL3* downregulation in human FFPE tissue specimen. (a) Quantification of *ebv-miR-BART7-3p* in human FFPE tissue specimen with known EBV status level. The expression of *ebv-miR-BART7-3p* was determined by qPCR and results are presented as relative expression of *ebv-miR-BART7-3p* in EBV-negative vs. EBV-positive cells. Representative EBER-ISH stainings of an EBV-positive (b) and EBV-negative (c) human tissue specimen (scale bar depicts 50 μ m). *IFNL3*-ISH stainings were performed in the same EBV-positive (d) and EBV-negative (e) human tissues (scale bar depicts 50 μ m) and the results were summarized (f). (g) The *IFNL3*-ISH signal was analyzed in *ebv-miR-BART7-3p* low- and high-expressing tissues (separated by median value, high ≥ 0.01 and low < 0.01 relative copy numbers).

The latent life cycle of EBV can be divided due to its gene expression profile into different latency phases. Latency 0 was found in infected and circulating memory B cells, latency 1 was typically observed in BL, latency 2 is characteristic for HL and NPC and latency phase 3 represents the B cell transformation.^{2,22,23} So far, the classification of these specific EBV life cycle phases is based on the expression profiles of long non-coding RNAs, e.g. EBER1 and EBER2, coding RNAs and even viral encoded peptides and proteins, but not on the expression profiles of the 48 virus-encoded miRs. Several EBV-encoded miRs, which are expressed not only during the lytic phase but also during different latent life cycle phases and thereby potentially participating in viral immune evasion, were identified.⁷ Ebv-miR-BART7-3p, but not all of the analyzed EBV miRs, exhibits very high expression levels in tonsils of acute mononucleosis patients representing the lytic life cycle as well as in EBV-positive NPCs, EBV-positive DLBCLs and EBV-positive BL cell lines representing different latent life cycle phases.⁷

Based on these results, ebv-miR-BART7-3p was selected as an interesting candidate for further target evaluation upon its overexpression. As a model system, HEK293T cells bearing the large T antigen and a plasmid containing an SV40 origin of replication were employed for ebv-miR-BART7-3p overexpression leading to expression levels comparable to that of *in vitro* EBV-positive BL cell lines. This vector-based expression system is less vulnerable to thaw-freeze cycles and to common RNA degradation, when compared to mimics, but causes the limitation that a single miR, namely hsa-miR-541, was used as a control instead of a scrambled mix potentially affecting transcriptome analyses.

Subsequent transcriptome analyses identified a strong impact on the expression of 234 endogenous human transcripts, not only limited to coding RNAs. Interestingly, ebv-miR-BART7-3p overexpression resulted in only a few upregulated transcripts. GO term enrichment analyses revealed that most of the deregulated transcripts belong to cellular processes, molecular binding and biological regulation. Indeed, ebv-miR-BART7-3p expression caused downregulation of anti-tumoral and anti-proliferative hsa-miR-34A by so far unknown indirect mechanisms. Furthermore, the downregulation of tumor-suppressive hsa-miR-34A per se is known to induce malignant transformation.²⁴ Due to the significant tumor suppressive effects of hsa-miR-34A, an hsa-miR-34A-based therapeutics has been developed, which already entered clinical trials (MRX34).²⁵

The direct interaction of the ebv-miR-BART7-3p expressed during the different EBV life cycle phases at high levels, with the IFNL3 mRNA clearly underlines the importance of this molecular mechanism contributing to immune evasion during latency and even during the lytic life cycle. IFNL3 is an essential component of the innate immune response to mucosal viral infections, in particular in the immune defense against clinically important viral pathogens, including influenza virus, norovirus and rotavirus.²⁶ A connection of IFNL3 with EBV has not yet been reported. However, the dsDNA virus EBV, which encodes miRs in contrast to RNA viruses, is able to efficiently neutralize IFNL3 before being able to induce its biological functions after translation. Future analyses should investigate putative sequence alterations within or close to the ebv-miR-

BART7-3p binding site within the IFNL3 gene and their potential role in disease progression. To achieve this, a more numerous, better balanced and perhaps more uniform human tissue cohort should be analyzed.

Due to the restricted expression of the IFNL3 respective receptor IL28R α /IFNLR1, the responses to IFNL3 in humans are generally limited to epithelial cells, peripheral blood lymphocytes, neutrophils and plasmacytoid DCs, with the major type III IFN responses occurring at the epithelial surfaces.²⁷ These reports further highlight IFNL3 as an essential target for the establishment of immune evasion by EBV, especially when epithelial cells of the oropharynx as well as cells of the tonsils, including naive and memory B cells, get infected for the first time. This study discovered one important molecular mechanism of ebv-miR-BART7-3p function, its direct binding to the 3'-UTR of IFNL3 mRNA as determined by luciferase reporter gene studies, which was accompanied by a downregulation of IFNL3 mRNA and/or protein both *in vitro* in EBV-positive B cell lymphoma cell lines and *in vivo* in human EBV-positive FFPE specimen.

Abbreviations

BART	BamHI-A rightward transcript
BHRF1	BamHI fragment H rightward open reading frame 1
BL	Burkitt's lymphoma
bp	base pair
CDS	coding sequence
cHL	classical Hodgkin lymphoma
DLBCL	diffuse large B cell lymphoma
DNA	deoxyribonucleic acid
dsDNA	double-stranded DNA
EBV	Epstein-Barr virus
EBER-CISH	Epstein-Barr virus-encoded RNA chromogenic in situ hybridization
ELISA	enzyme-linked immunosorbent assay
ENKTL	extranodal NK/T cell lymphoma
FFPE	formalin fixed paraffin embedded
GC	gastric adenocarcinoma
HHV	human herpes virus
HLA	human leukocyte antigen
IFN	interferon
IL	interleukin
ISH	in situ hybridization
MCS	multiple cloning site
MFI	mean fluorescence intensity
miR	microRNA
mPTLD	monomorphic post-transplant lymphoproliferative disorder
NHL	non-Hodgkin lymphoma
NPC	nasopharyngeal carcinoma
nt	nucleotide
qPCR	quantitative polymerase chain reaction
RNA	ribonucleic acid
Treg	regulatory T cell
UTR	untranslated region
WHO	World Health Organization

Acknowledgments

We thank Prof. Michael Bachmann (Helmholtz-Zentrum Dresden Rossendorf, Institute of Radiopharmaceutical Cancer Research Dresden, Germany) for his support and Maria Heise for excellent secretarial help.

Disclosure statement

No potential conflict of interest was reported by the author(s).

Funding

This article was supported by grants from the German Research Foundation (DFG; project numbers: 496182670 SJB; SE581/34-1 BS), the Jackstädt Foundation (SJB), the Monika Kutzner Foundation (SJB), the German Israeli Foundation (GIF I-1412-414.13-2017; BS, OM) and the BMBF (ZB 031B0800B CW, BS). Funded by the Brandenburg Medical School publication fund supported by the Ministry of Science, Research and Cultural Affairs of the State of Brandenburg.

Author contributions

SJB designed the project and is responsible for the study. Material preparation, data collection including clinical parameters and analysis were performed by MB, CW, AW, JB and SJB. Experimental work was performed by JB, MB, SJB and CV, and the results and their interpretation were discussed by JB, SJB, MB and BS. The first draft of the manuscript was written by SJB, JB, MB and BS. SJB, JB, MB and CV prepared the figures. SJB, CW, OM and BS revised the final version of the manuscript, which was approved by all authors.

Data availability statement

The authors confirm that the data supporting the findings of this study are available within the article and/or its supplementary materials.

References

- Dunmire SK, Verghese PS, Balfour HH Jr. Primary Epstein-Barr virus infection. *J Clin Virol.* 2018;102:84–92. doi:10.1016/j.jcv.2018.03.001.
- Bauer M, Jasinski-Bergner S, Mandelboim O, Wickenhauser C, Seliger B. Epstein-Barr Virus—Associated Malignancies and Immune Escape: The Role of the Tumor Microenvironment and Tumor Cell Evasion Strategies. *Cancers Basel.* 2021;13(20):5189. doi:10.3390/cancers13205189.
- Pathmanathan R, Prasad U, Sadler R, Flynn K, Raab-Traub N. Clonal proliferations of cells infected with Epstein-Barr virus in preinvasive lesions related to nasopharyngeal carcinoma. *N Engl J Med.* 1995;333(11):693–698. doi:10.1056/NEJM199509143331103.
- Shibata D, Weiss LM. Epstein-Barr virus-associated gastric adenocarcinoma. *Am J Pathol.* 1992;140:769–774.
- Huang X, Nolte I, Gao Z, Vos H, Hepkema B, Poppema S, van den Berg A, Diepstra A, Zhang L. Epidemiology of classical Hodgkin lymphoma and its association with Epstein Barr virus in Northern China. *PLoS ONE.* 2011;6(6):e21152. doi:10.1371/journal.pone.0021152.
- Ogwang MD, Bhatia K, Biggar RJ, Mbulaiteye SM. Incidence and geographic distribution of endemic Burkitt lymphoma in northern Uganda revisited. *Int J Cancer.* 2008;123(11):2658–2663. doi:10.1002/ijc.23800.
- Jasinski-Bergner S, Blumke J, Bauer M, Skiebe SL, Mandelboim O, Wickenhauser C, Seliger B. Novel approach to identify putative Epstein-Barr-virus microRNAs regulating host cell genes with relevance in tumor biology and immunology. *Oncoimmunology.* 2022;11(1):2070338. doi:10.1080/2162402X.2022.2070338.
- Jasinski-Bergner S, Mandelboim O, Seliger B. Molecular mechanisms of human herpes viruses inferring with host immune surveillance. *J Immunother Cancer.* 2020;8(2):e000841. doi:10.1136/jitc-2020-000841.
- Thorley-Lawson DA. EBV persistence—introducing the virus. *Curr Top Microbiol Immunol.* 2015;390(Pt 1):151–209.
- Xia T, O'Hara A, Araujo I, Barreto J, Carvalho E, Sapucaia JB, Ramos JC, Luz E, Pedrosa C, Manrique M, et al. EBV microRNAs in primary lymphomas and targeting of CXCL-11 by ebv-mir-BHRF1-3. *Cancer Res.* 2008;68(5):1436–1442. doi:10.1158/0008-5472.CAN-07-5126.
- Albanese M, Tagawa T, Bouvet M, Maliqi L, Lutter D, Hoser J, Hastreiter M, Hayes M, Sugden B, Martin L, et al. Epstein-Barr virus microRNAs reduce immune surveillance by virus-specific CD8 + T cells. *Proceedings of the National Academy of Sciences USA.* 2016;113(42):E6467–E6475. doi:10.1073/pnas.1605884113.
- Jasinski-Bergner S, Stoehr C, Bukur J, Massa C, Braun J, Huttelmaier S, Spath V, Wartenberg R, Legal W, Taubert H, et al. Clinical relevance of miR-mediated HLA-G regulation and the associated immune cell infiltration in renal cell carcinoma. *Oncoimmunology.* 2015;4(6):e1008805. doi:10.1080/2162402X.2015.1008805.
- Jasinski-Bergner S, Reches A, Stoehr C, Massa C, Gonschorek E, Huttelmaier S, Braun J, Wach S, Wullich B, Spath V, et al. Identification of novel microRNAs regulating HLA-G expression and investigating their clinical relevance in renal cell carcinoma. *Oncotarget.* 2016;7(18):26866–78.
- Jasinski-Bergner S, Mandelboim O, Seliger B. The role of microRNAs in the control of innate immune response in cancer. *J Natl Cancer Inst.* 2014;106(10): doi:10.1093/jnci/dju257.
- Chen C, Ridzon DA, Broomer AJ, Zhou Z, Lee DH, Nguyen JT, Barbisin M, Xu NL, Mahuvakar VR, Andersen MR, et al. Real-time quantification of microRNAs by stem-loop RT-PCR. *Nucleic Acids Res.* 2005;33(20):e179. doi:10.1093/nar/gni178.
- WHO classification of tumours of haematopoietic and lymphoid tissues, NLM ID: 101716000, ISBN: 9789283244943.
- WHO Classification of Head and Neck Tumours. WHO/IARC classification of tumours. Vol. 9. 4th ed. 2017.
- Wu X, Cheng YL, Matthen M, Yoon A, Schwartz GK, Bala S, Taylor AM, Momen-Heravi F. Down-regulation of the tumor suppressor miR-34a contributes to head and neck cancer by up-regulating the MET oncogene and modulating tumor immune evasion. *J Exp Clin Cancer Res.* 2021;40(1):70. doi:10.1186/s13046-021-01865-2.
- Andreaskos E, Salagianni M, Galani IE, Koltsida O. Interferon- λ s: Front-line Guardians of Immunity and homeostasis in the respiratory tract. *Front Immunol.* 2017;8:1232. doi:10.3389/fimmu.2017.01232.
- Rosa F, Berissi H, Weissenbach J, Maroteaux L, Fellous M, Revel M. The beta2-microglobulin mRNA in human Daudi cells has a mutated initiation codon but is still inducible by interferon. *EMBO J.* 1983;2(2):239–243. doi:10.1002/j.1460-2075.1983.tb01412.x.
- Rehmsmeier M, Steffen P, Hochsmann M, Giegerich R. Fast and effective prediction of microRNA/target duplexes. *RNA.* 2004;10(10):1507–1517. doi:10.1261/rna.5248604.
- Tierney RJ, Shannon-Lowe CD, Fitzsimmons L, Bell AI, Rowe M. Unexpected patterns of Epstein-Barr virus transcription revealed by a high throughput PCR array for absolute quantification of viral mRNA. *Virology.* 2015;474:117–130. doi:10.1016/j.virol.2014.10.030.
- Kang MS, Kieff E. Epstein-Barr virus latent genes. *Experimental & Molecular Medicine.* 2015;47(1):e131. doi:10.1038/emm.2014.84.
- Yamamura S, Saini S, Majid S, Hirata H, Ueno K, Chang I, Tanaka Y, Gupta A, Dahiya R. MicroRNA-34a suppresses malignant transformation by targeting c-Myc transcriptional complexes in human renal cell carcinoma. *Carcinogenesis.* 2012;33(2):294–300. doi:10.1093/carcin/bgr286.

25. Hong DS, Kang YK, Borad M, Sachdev J, Ejadi S, Lim HY, Brenner AJ, Park K, Lee JL, Kim TY, et al. Phase 1 study of MRX34, a liposomal miR-34a mimic, in patients with advanced solid tumours. *Br J Cancer*. 2020;122(11):1630–1637. doi:10.1038/s41416-020-0802-1.
26. Peterson ST, Kennedy EA, Bringleb PH, Taylor GM, Urbanek K, Bricker TL, Lee S, Shin H, Dermody TS, Boon ACM, et al. Disruption of type III interferon (IFN) genes *Ifnl2* and *Ifnl3* recapitulates loss of the type III IFN receptor in the mucosal antiviral response. *J Virol*. 2019;93(22). doi:10.1128/JVI.01073-19.
27. Walker FC, Sridhar PR, Baldrige MT. Differential roles of interferons in innate responses to mucosal viral infections. *Trends Immunol*. 2021;42(11):1009–1023. doi:10.1016/j.it.2021.09.003.